Characterization of Basalt FRP Compared to Glass FRP Bars

Hesham Sokairge[1], Fareed Elgabbas[2], Hany Elshafie[3]

Abstract— The great evolution in composite materials have arisen the need for developing new types of fibers that can offers better distinguished properties with reasonable cost. Basalt fiber reinforced polymer (BFRP) is a new generation of FRP composites that have been announced in the last decade. This study presents an experimental investigation of the physical and mechanical properties of BFRP bars compared to glass FRP (GFRP) bars. The type of fibers (Basalt and Glass), the bar diameter (6 mm and 10 mm), and the fiber volume fraction (65% and 50%), which arises from investigating of physical properties, were the variables considered in this study. Based on the test results, the BFRP bars of same fiber volume fraction compared to GFRP bars showed significant better mechanical properties of about 1.7 times that of GFRP bars. Moreover, the fiber volume fraction has been proved to have a great impact on the mechanical properties in addition to improving the creep behavior of BFRP bars. The million-hour creep rupture stress of BFRP bars was analyzed and limited to 63.3% and 56.7% for 6 mm and 10 mm diameter BFRP bars, respectively, of fiber volume fraction 65% and 50%, respectively. Consequently, BFRP bars is recommended to be used in prestressing applications and gain higher priority compared to GFRP bars.

INDEX TERMS— Basalt Fiber Reinforced Polymer; Fiber Content; Tensile Strength; Creep Rupture.

1. INTRODUCTION

FRP bars have been used as alternative to traditional steel rebars in construction field for decades owing to their noncorrosive nature, light weight, high specific strength and stiffness [1]. Although, carbon FRP bars are much stiffer than glass FRP and have elastic modulus similar to that of steel. Nevertheless, glass FRP bars have gained a large share of manufacturers' interest and long established availability on markets owing to its low cost specially in mass applications [2]. The recent attempts for developing the FRP composites in construction field is devoted towards introducing new types of fibers which can offer better characteristics with comparable cost to commonly known glass, aramid, and carbon fibers [3]. BFRP composite is a new generation of FRP composite materials that have been recently introduced to composites markets as a strong alternative to GFRP composites with competing price. Unlike glass fibers, basalt fibers are manufactured from single phase process of fusing basalt rocks with no need for additional secondary materials [4]. This simplification in the manufacturing process results in low production cost compared to other types of fibers [5], in addition to being natural green fibers and environmental friendliness owing to saving energy during manufacture [6].

Although basalt fibers are similar in chemical composition to asbestos fibers, but basalt fibers are considered safe due to their different morphology and surface properties that suppress toxic effect presented in asbestos [7]. Basalt FRP composites are expected to offer many distinguished properties with competing price. However, the available researches on the characterization of BFRP are still limited and BFRP are still not included in design guidelines. Consequently, the physical and mechanical properties of BFRP bars will be evaluated in this study compared to GFRP bars as step for introducing BFRP to design guidelines.

2. EXPERIMENTAL PROGRAM

This study aimed at investigating two types of FRP bars, BFRP bars of 6 mm and 10 mm nominal diameter, and GFRP bars of 10 mm nominal diameter, as shown in Figure 1. The physical properties were determined as a characterization of the tested FRP bars in order to highlight any variables that could affect the mechanical properties test results. The physical properties (cross sectional properties, relative density, and fiber volume fraction) and mechanical properties (Tension, transverse shear, flexure, interlaminar shear, and tensile creep rupture) of the FRP bars were tested according to [8] and the relevant ASTM standards [9], [10], [11], [12], [13], [14], [15]. Table 1 summarize the test matrix.

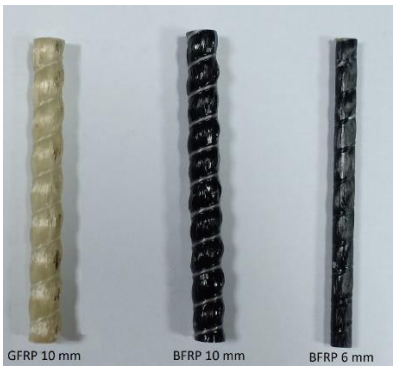

Figure 1: Tested basalt and glass FRP bars

Table 1: Experimental Program Test Matrix

1 *Teaching Assistant, Hesham Sokairge, Structural Engineering Department, Faculty of Engineering, Ain shams University, Egypt. E-mail: h_sokairge@eng.asu.edu.eg*
2 *Assistant Professor, Fareed Elgabbas, Structural Engineering Department, Faculty of Engineering, Ain shams University, Egypt. E-mail: Fareed.Elgabbas@eng.asu.edu.eg*
3 *Professor, Hany Elshafie, Structural Engineering Department, Faculty of Engineering, Ain shams University, Egypt. E-mail: Hany.elshafie@eng.esu.edu.eg*

General Properties	Specified Property	FRP Bar Type	Diameter (mm)	No. of Specimens	Standards
Physical Properties	Cross Section Properties	BFRP	6	5	ACI 440.3R [8]
			10		
		GFRP	10		
	Relative Density	BFRP	6		ASTM D792 [9]
			10		
		GFRP	10		
	Fiber Content	BFRP	6	1	ASTM D3171 [10]
			10		
		GFRP	10		
Mechanical Properties	Tensile	BFRP	6	5	ASTM D7205 [11]
			10		
		GFRP	10		
	Flexural	BFRP	6		ASTM D4476 [13]
			10		
		GFRP	10		
	Interlaminar shear	BFRP	6		ASTM D4475 [14]
			10		
		GFRP	10		
	Transvers Shear	BFRP	6		ASTM D7617 [12]
			10		
		GFRP	10		
	Creep Rupture	BFRP	6	3	ASTM D7337 [15]
			10		

3. Test Setup and Calculations

3.1 Cross-Sectional Properties of FRP Bars

To assess the uniformity and quality of manufacturing process the cross-sectional properties of FRP bars were evaluated. Five FRP bars' specimens of length 200 mm from each type and each diameter were tested in accordance with [8] by measuring their length accurately through taking the average of three different measurements spanning 120 degree along the permitter of the bar then measuring their volume through immersing in water. Finally, the specimens' cross-sectional properties were calculated as follow:

a) Cross-sectional Area:

$$A_f = \frac{V}{L_a} \quad (1)$$

b) Equivalent Diameter:

$$d_b = 2\sqrt{\frac{A_f}{\pi}} \quad (2)$$

c) Equivalent Circumference:

$$C_b = d_b * \pi \quad (3)$$

3.2 Relative Density of BFRP Bars

In order to identify the material uniformity degree and as a secondary test for determining the fiber volume fraction of presented FRP bars, the relative density was measured. Five FRP bars' specimens of each type and each diameter were tested according to [9] by measuring their weight in air and after submerging in water. Then the density was calculated as follow:

$$\text{Specific gravity} = \frac{a}{a-b} \quad (4)$$

$$\text{Density} = \text{Specific gravity} \times 997.5 \quad (5)$$

3.3 Fiber Content of FRP Bars

Identifying the constituent content is one of the major factors used in characterization of FRP composites as it is used in analytical modeling of the composite properties and assessing the quality of production process. Moreover, it is used in the normalization of the mechanical properties of the composite material. Three specimens, GFRP bar of diameter 10 mm, and BFRP bars of 6 mm and 10 mm diameter, were test for identifying the fiber volume fraction according to [10]. Specimens of length 20 mm were cut and weighted, then placed into suitable beaker containing 50 ml of 70 % nitric acid. Then, the beakers were heated on hot plate until the matrix is fully digested for about 6 hours, as shown in Figure 2**Error! Reference source not found.**. The specimens were washed using distilled water before heating in oven for one hour at 100 °C. Finally, the specimens were cooled and weighted again, as shown in Figure 3, and the fiber content were determined as follow:

$$V_r = \left(M_f/M_i\right) \times 100 \times (\rho_c/\rho_r) \quad (6)$$

Figure 2: Basalt and Glass FRP tested specimens placed in 70% nitric acid then heated

Figure 3: Remaining basalt and glass fibers after testing

3.4 Tensile Properties of FRP Bars

The tensile properties of FRP bars are considered the most important property which differentiate between various types of FRP bars. Five FRP bars' specimens of each diameter from each bar type were tested in a static tensile test according to [11]. The tested specimens have 1000 mm total length and 400 mm free length. For BFRP and GFRP bars of 10 mm diameter, steel tubes of length 310 mm and filled with epoxy resin of thickness 6 mm surrounding the FRP bars, were used for facilitating gripping in the universal testing machine. Four hollow PVC rings were used for fitting the bar position concentric with anchoring tubes. A universal testing machine of capacity 200 kN and sensitivity 0.5 kN was used for testing the FRP bars' specimens. The elongation of each specimen was measured through attaching two dial gages of capacity 35 mm and sensitivity 0.005 mm to the specimens with a gage length of 200 mm. Figure 4 shows the tension test setup and typical failure mode. The tensile properties of tested FRP bars were calculated as follow:

a) Tensile Strength:

$$f_u = \frac{T_u}{A} \quad (7)$$

b) Modulus of Elasticity:

$$E_f = \frac{\Delta\sigma}{\Delta\varepsilon} \quad (8)$$

c) Ultimate Tensile Strain:

$$\varepsilon_u = \frac{L_i - L_o}{L_o} \quad (9)$$

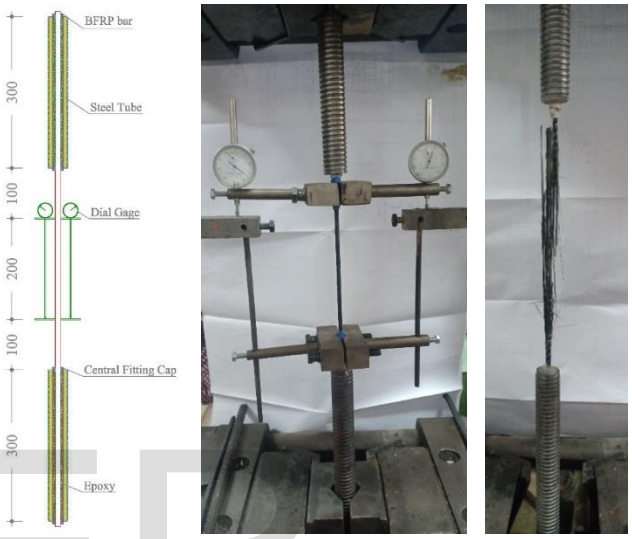

Figure 4: Tension test setup and typical failure mode

3.5 Flexural Strength of FRP Bars

The flexural strength of available FRP bars were assessed as part of their characterization and a part of the comparative study. Five FRP bars' specimens from each diameter of each bar type were tested according to [13]. Specimens of length 20 times the bar diameter were tested under one-point loading flexural test up to failure, as show in Figure 5. The clear span was set to 18 times the bar diameter. The specimens were tested in universal testing machine of capacity 50 kN. All the specimens failed by tensile fracture of outer fibers in the tension side. The flexural strength of tested specimens was calculated as follow:

$$S_f = \frac{P_f L_f C}{4I} \quad (10)$$

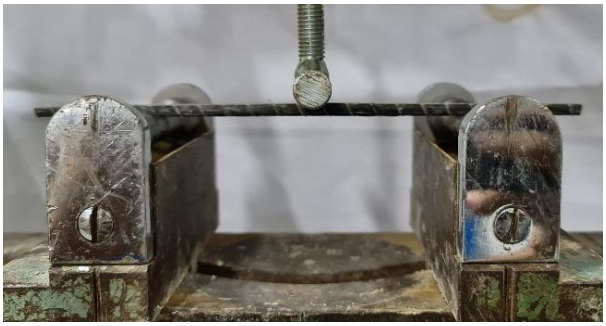

Test setup

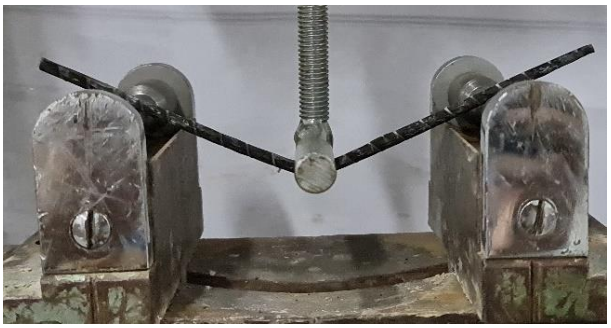

BFRP bars of 6 mm diameters

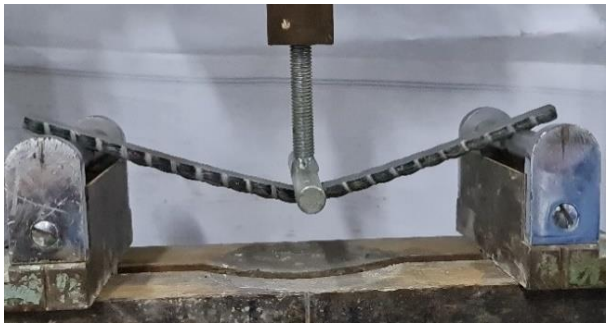

BFRP bars of 10 mm diameters

GFRP bars of 10 mm diameters

Figure 5: Flexural test setup and typical failure mode

3.6 Transverse Shear Strength of FRP Bars

Five FRP bars' specimens of each type from each diameter were tested according to [12] as a part of the comparative study. Specimens of length 200 mm were probably cut and fitted into double shear apparatus with appropriate cutting blade. The apparatus was placed in a universal testing machine and monotonically loaded up to failure, as shown in Figure 6. The transverse shear strength was calculated as follow:

$$\tau_u = \frac{P_S}{2A} \quad (11)$$

Test Setup

BFRP bars of 6 mm diameters

BFRP bars of 10 mm diameters

GFRP bars of 10 mm diameters

3.7 Interlaminar Shear Strength of FRP Bars

The horizontal stresses arise between unidirectional fibers manufactured using pultrusion process and resin matrix in FRP bars induce interface deterioration higher than transvers shear stresses [16]. Accordingly, the apparent horizontal shear strength (Interlaminar shear strength) of the available FRP bars were assessed using short beam test method according to [14]. Five specimens from each diameter of each bar type were used in this investigation. The specimens were of length 5 times the bar diameter. The specimens were tested in bending configuration with clear span of 3 times the bar diameter. The specimens were center loaded up to failure, as shown in Figure 7. The apparent horizontal shear strength was calculated as follow:

$$S = 0.849\frac{P_{is}}{d^2} \quad (12)$$

Test Setup

BFRP bars of 6 mm diameters

BFRP bars of 10 mm diameters

GFRP bars of 10 mm diameters

Figure 7: Short beam test setup and typical failure mode.

3.8 Creep Rupture Strength of FRP Bars

The creep rupture strength is one of the main properties that affect the use of FRP bars in prestressing applications. GFRP bars were excluded from being used in prestressing application due to their low creep rupture stress of 30% of the ultimate tensile strength. Consequently, in this study the creep rupture strength of BFRP bars were investigated and the creep rupture strength after million-hour was extrapolated based on statical analysis of the experimental results. A total of six BFRP bars were tested in creep test, three specimens for each. The specimens were of length 1200 mm and prepared following the same procedures of tensile strength test. The specimens were tested following the test procedures recommended by [15]. All the specimens were subjected to initial sustained stress using creep frame shown in Figure 8, and the creep strain was monitored with time up to failure. A sustained stress ratio of 75%, 72.5%, and 70.0% were used for 6 mm diameter BFRP bars, while 70%, 67.5%, and 65% sustained stress ratios were used for 10 mm diameter BFRP bars. The sustained stress level resulted from trial-and-error procedures to achieve certain criteria of having rupture time of three specimens spanning three different decades of time including 10, 100, and 1000 hours to allow for initiation of linear regression based on reasonable data.

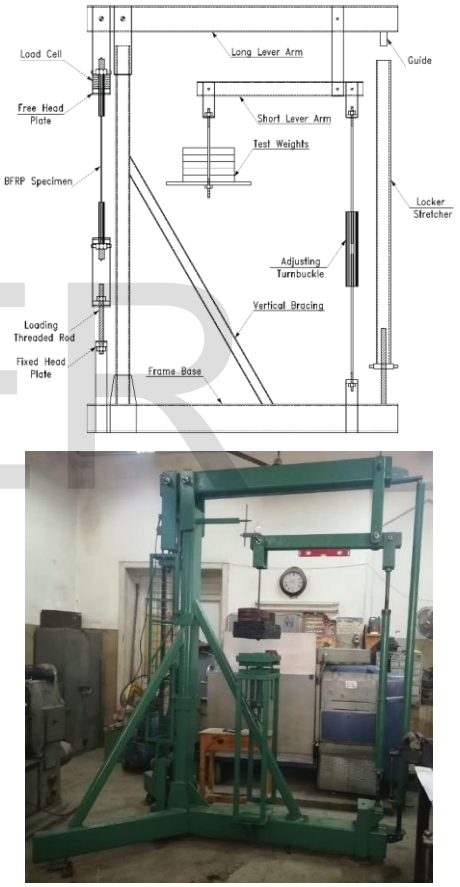

Figure 8: Creep test setup

4. Results and Discussion

4.1 Physical Properties

As mentioned previously, the physical properties were assessed as a part of material characterization and to introduce any variables that are not considered in this study. The physical properties were evaluated and calculated based on the previously mentioned tests' procedures and the results are reported in Table 2.

Table 2: Physical Properties of FRP Bars

Property	BFRP		GFRP
Nominal diameter (mm)	6	10	10
Cross-sectional Area (mm^2)	31.15±1.23	80.13±1.99	82.85±1.21
Equivalent diameter (mm)	6.30±0.12	10.10±0.13	10.27±0.08
Equivalent circumference (mm)	19.78±0.39	31.73±0.39	32.27±0.24
Density (kg/m^3)	1951.8±19.4	1853.7±31.3	1891.3±19.3
Fiber Volume Fraction (%)	65	50	65

Based on the previously mentioned test results, the BFRP and GFRP bars showed a reasonable standard deviation reflecting the uniformity and quality of manufacturing process. Moreover, the test results demonstrated the presence of additional variable that should be considered in this study presented in the different fiber volume fraction of available FRP bars, such that the fiber volume fraction of 6 mm and 10 mm diameter BFRP bars were 65% and 50%, respectively, while the fiber volume fraction of 10 mm diameter GFRP bars was 65%.

4.2 Short-Term Mechanical Properties

The short-term mechanical properties of BFRP and GFRP bars were tested and calculated based on the previously mentioned tests' procedures and the results are summarized in Table 3. Based on the test results, BFRP bars of 10 mm diameter showed slight enhanced mechanical properties compared to GFRP bars. Nevertheless, the lower fiber volume fraction of 10 mm diameter BFRP bars compared to that of GFRP bars gives an indication of better mechanical properties of BFRP bars. On the other hand, BFRP bars of 6 mm diameter showed higher mechanical properties compared to that of 10 mm diameter BFRP bars. This is attributed to the higher fiber volume fraction of 6 mm diameter BFRP bars compared to that of 10 mm diameter BFRP bars. Moreover, BFRP bars of 6 mm diameter showed higher tensile strength, flexural strength, transvers shear strength, and interlaminar shear strength about 1.64, 1.45, 2.14, and 1.47, respectively times that of GFRP bars of same fiber volume fraction. Consequently, the test results demonstrated that BFRP bars offers higher mechanical properties compared to that of GFRP bars of same fiber volume fraction with a competing price, in addition to the simplicity of its manufacturing process and being environmental friendless. All these advantages give BFRP the priority over GFRP bars in construction and strengthening field.

Table 3: Short-Term Mechanical Properties of FRP Bars

Property	BFRP		GFRP
Nominal diameter (mm)	6	10	10
Tensile strength (MPa)	1570.3±45	986.78±16	925.54±21
Modulus of elasticity (GPa)	60.33±1.5	39.192±0.7	39.436±0.2
Ultimate strain (%)	2.60±0.12	2.518±0.07	2.352±0.05
Flexural strength (MPa)	1785.3±73	1307.6±58	1229.3±57
Transverse shear strength (MPa)	313.54±8.0	148.33±6.7	146.55±3.2
Interlaminar shear strength (MPa)	67.45±2.27	52.81±1.71	45.85±0.67

* The mechanical properties were calculated based on the nominal diameter.

4.3 Long-Term Creep Rupture Strength

In this study the creep rupture strength of BFRP bars was investigated as an important factor specially for prestressing applications. Table 4 reports the creep test results of tested specimens, while Figure 9 and Figure 10 present the test results in the form of creep tensile strain with respect to time for 6 mm and 10 mm diameter BFRP bars, respectively. Based on the test results, BFRP bars showed similar creep behavior compared to other types of FRP bars by following the three phases of creep behavior. The first phase was characterized by high strain rate decreasing gradually until reaching second phase within limited period compared to test time. The second phase was characterized by a slow strain rate within a long period until reaching the third phase where the strain rate increased rapidly with successive fracture of fibers up to fracture of BFRP bars. Additionally, the test results demonstrated the impact of fiber volume fraction on the creep rupture strength of BFRP bars, such that the creep rupture stress of 6 mm diameter BFRP bars were higher than that of 10 mm diameter BFRP bars which failed within the same time decade. Furthermore, based on the test results, the million-hour creep rupture strength of 6 mm and 10 mm diameter BFRP bars were predicted by extrapolation using linear regression as shown in Figure 11 and were set to 63.3% and 56.7%, respectively.

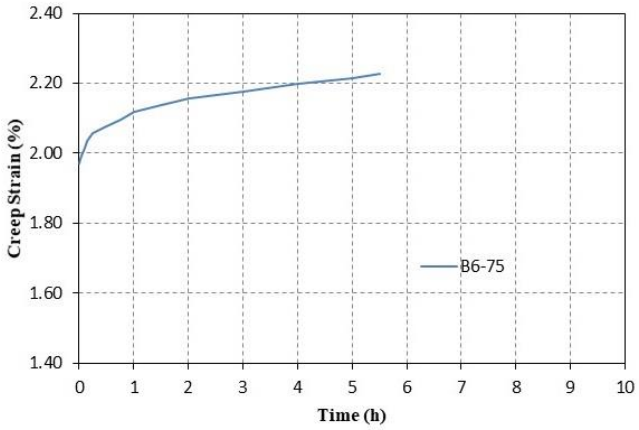

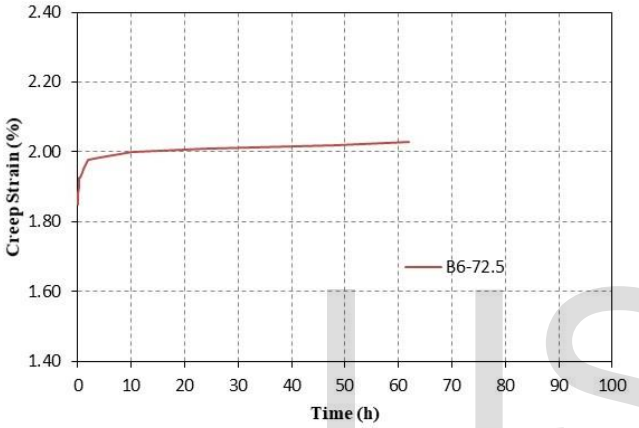

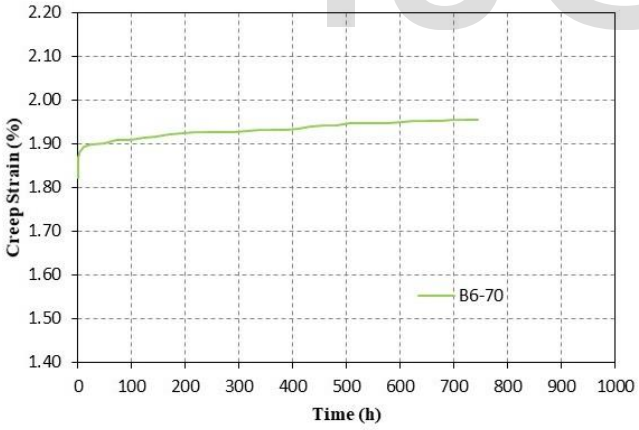

Figure 9: Creep tensile strain versus time for 6 mm BFRP bars

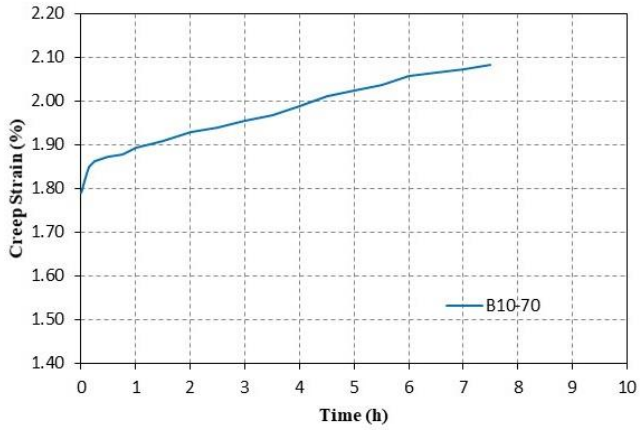

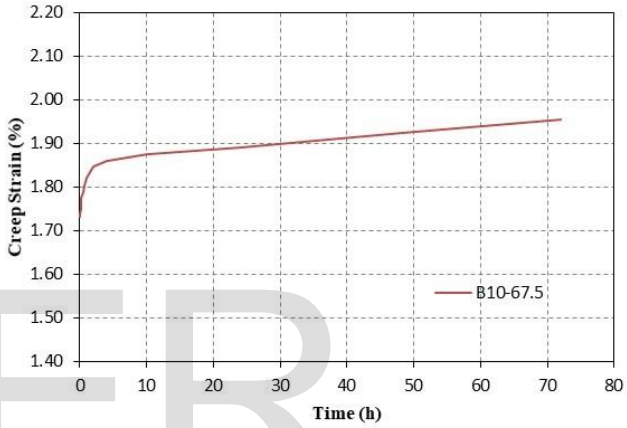

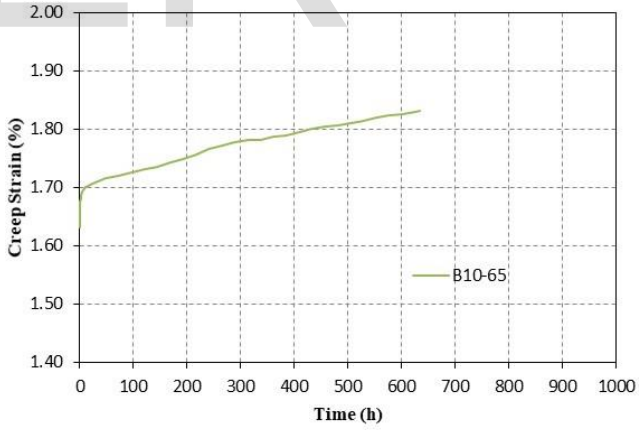

Figure 10: Creep tensile strain versus time for 10 mm BFRP bars

Table 4: Creep Test Results

Code	Initial Stress Level (%)	Initial Strain "ε_i" (%)	Strain at End of 2nd Stage "ε_f" (%)	Creep Strain "$\Delta\varepsilon$" (%)	Rupture Period (h)
B6-75	75.0	1.97	2.228	0.258	5.5
B6-72.5	72.5	1.85	2.027	0.177	62
B6-70	70.0	1.82	1.953	0.133	744
B10-70	70.0	1.79	2.081	0.331	7.5
B10-67.5	67.5	1.73	1.954	0.224	72
B10-65	65.0	1.63	1.825	0.195	634

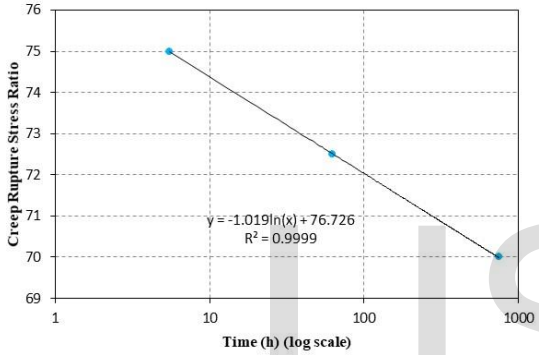

6 mm diameter BFRP bars

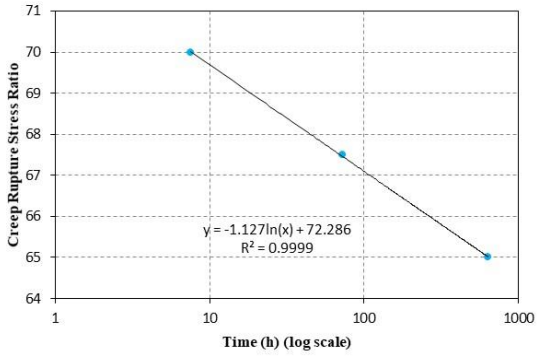

10 mm diameter BFRP bars

Figure 11: The initial stress ratio versus creep rupture time for 6 mm and 10 mm diameter BFRP bars

5. Conclusions

This research presents a comparative study between the short- and long-term mechanical properties of BFRP and GFRP bars. The bar diameter, type of fibers, and fiber volume fraction were the variables considered in this study. Based on the test results, the following conclusions can be drawn:

- The BFRP bars of similar fiber volume fraction to GFRP bars offer higher mechanical properties about 1.7 times that of GFRP bars with approximately same cost.
- The fiber volume fraction has a great impact on the mechanical properties of BFRP bars.
- BFRP bars showed linear relationship between creep rupture stress and logarithm of time similar to other types of FRP bars.
- The fiber volume fraction has a significant impact on the creep rupture strength of BFRP bars.
- BFRP bars offer high creep rupture stress which gives it additional advantage in prestressing application compared to GFRP bars.
- Base on extrapolation of test results using linear regression analysis, the million-hour creep rupture strength of BFRP bars is limited to 63.3% and 56.7% for BFRP bars of 65% and 55% fiber volume fraction, respectively.

Nomenclature

A_f	=	cross-sectional area of the FRP bars (mm²)
a	=	apparent mass of specimen (g)
b	=	apparent mass of specimen completely immersed in water (g)
C	=	distance from centroid to extremities (mm)
C_b	=	Equivalent Circumference of tested specimen (mm)
d	=	specimen diameter (mm)
d_b	=	Equivalent diameter of tested specimen (mm)
I	=	moment of inertia (mm4)
L_a	=	average length of the tested specimen (mm)
L_f	=	support span (mm)
L_i	=	gauge length after loading (mm)
L_o	=	initial gage length (mm)
M_f	=	final mass of the specimen after digestion (g)
M_i	=	initial mass of the specimen (g)
P_f	=	ultimate flexural force (N)
P_{is}	=	Interlaminar shear ultimate load (N)
P_s	=	maximum shear force (N)
S	=	apparent horizontal shear strength (MPa)
S_f	=	flexural stress in outer fibers at midspan (MPa)
T_u	=	ultimate tensile load (N)

V = volume of the tested specimen (mm^3)

V_r = fiber volume fraction (%)

$\Delta\varepsilon$ = average strain corresponding to the measured stress

ρ_c = density of FRP specimen (g/mm^3)

ρ_r = density of fibers (g/mm^3)

$\Delta\sigma$ = difference between applied stress at 25% and 75% of ultimate stress (MPa)

τ_u = transverse shear strength (MPa)

6. REFERENCES

[1] ACI Committee 440.2R, Guide for the Design and Construction of Externally Bonded FRP Systems for Strengthening Concrete Structures, American concrete institute, Farmington Hills, MI., 2017.

[2] F.C. Campbell, Structural Composite Materials, ASM Interational, 2010.

[3] F. Elgabbas, E.A. Ahmed, B. Benmokrane, Physical and mechanical characteristics of new basalt-FRP bars for reinforcing concrete structures, Constr. Build. Mater. 95 (2015) 623–635. doi:10.1016/j.conbuildmat.2015.07.036.

[4] K. Singha, A Short Review on Basalt Fiber, Int. J. Text. Sci. 1 (2012) 19–28. doi:10.5923/j.textile.20120104.02.

[5] V. Ramakrishnan, R. Panchalan, A new construction Material—Non-corrosive basalt bar reinforced concrete, Spec. Publ. 229 (2005) 253–270.

[6] W. Zhishen, W. Xin, W. Gang, Advancement of structural safety and sustainability with basalt fiber reinforced polymers, in: CICE 6th Int. Conf. FRP Compos. Civ. Eng., International Institute for FRP in Construction (IIFC), Rome, Italy, 2012: pp. 15–29.

[7] E. Quagliarini, F. Monni, S. Lenci, F.B.-C. and Building, undefined 2012, Tensile characterization of basalt fiber rods and ropes: A first contribution, Elsevier. (n.d.).

[8] ACI Committee 440.3R, Guide Test Methods for Fiber-Reinforced Polymers (FRPs) for Reinforcing or Strengthening Concrete Structures, 2012.

[9] ASTM D792, Standard Test Methods for Density and Specific Gravity (Relative Density) of Plastics by Displacement, Am. Soc. Test. Mater. (2013) 6. doi:10.1520/D0792-13.2.

[10] ASTM D3171, Standard Test Methods for Constituent Content of Composite Prepreg 1, Am. Soc. Test. Mater. (2015). doi:10.1520/D3171-15.2.

[11] ASTM D7205 / D7205M-06(2016), Standard Test Method for Tensile Properties of Fiber Reinforced Polymer Matrix Composite Bars, Am. Soc. Test. Mater. (2016). doi:10.1520/D7205_D7205M-06R16.

[12] ASTM D7617 / D7617M, Standard Test Method for Transverse Shear Strength of Fiber-reinforced Polymer Matrix Composite Bars, Am. Soc. Test. Mater. (2017). doi:10.1520/D7617.

[13] ASTM D4476, Standard Test Method for Flexural Properties of Fiber Reinforced Pultruded Plastic, Am. Soc. Test. Mater. (2014). doi:10.1520/D4476.

[14] ASTM D4475, Standard Test Method for Apparent Horizontal Shear Strength of Pultruded Reinforced Plastic Rods By the Short-Beam Method, Am. Soc. Test. Mater. (2016). doi:10.1520/D4475-02R16.2.

[15] ASTM D7337/D7337M, Standard Test Method for Tensile Creep Rupture of Fiber Reinforced Polymer Matrix, Am. Soc. Test. Mater. (2012). doi:10.1520/D7337.

[16] C.G. Park, C. Il Jang, S.W. Lee, J.P. Won, Microstructural investigation of long-term degradation mechanisms in GFRP dowel bars for jointed concrete pavement, J. Appl. Polym. Sci. 108 (2008) 3128–3137. doi:10.1002/app.27946.